

References and Notes

- In the change of perspective from lunar orbit to the earth's surface as observing station, the angular size of the moon in the field of view is greatly reduced. But a nearly negligible change in the very much greater distance to the sun occurs, so that the mapping of phase angle onto the sky as circles concentric about the antisolar direction is unaffected in scale. (The local phase angle of an observed landmark is the angle between the observer and the sun as it would be measured from that landmark.)
- The Heiligenschein region of the lunar photometric function was first detected from the earth in 1964 by T. Gehrels, T. Coffeen, and D. Owings [*Astron. J.* 69, 826 (1964)], wherein it was referred to as the "opposition effect," and also, but at a lower signal-to-noise ratio, by R. Wildey and H. Pohn (*ibid.*, p. 619); see also J. Van Diggelen, *Planet. Space Sci.* 13, 271 (1965). Direct observation of the entire eclipsed region based on the use of Apollo orbital photography was carried out by H. Pohn, H. Radin, and R. Wildey [*Astrophys. J.* 157, L193 (1969)]. Although the angular spread of the earth is greater than that of the sun as seen from the moon, the angular spread of the Apollo command module is negligible compared to that of the sun and is a negligible source of obscuration and diffraction when seen from the moon in transit on the solar disk. R. Wildey and H. Pohn [*Astrophys. J.* 158, L129 (1969)] by similar methods confirmed that the magnitude of the effect was variable over the lunar surface. Laboratory studies of the optical properties of Apollo-returned samples by B. O'Leary and F. Briggs [*J. Geophys. Res.* 75, 6532 (1970); *ibid.* 78, 792 (1973)] confirmed and extended these studies.
- The relevant scale of roughness a priori includes all radii of surface curvature in the range from just below resolution (a few hundred meters at astronomical resolution or a few meters at Apollo resolution) to just above the wavelength of light, or about 1 μm . In practical terms, the effective range of the size distribution of soil particles (tens to hundreds of micrometers) is strongly dominant. The existence of the Heiligenschein phenomenon is then implied by the disappearance of visible shadows at a phase angle of zero. For explicitly quantitative theories of the effect, see B. Hapke [*J. Geophys. Res.* 68, 4571 (1963); *Astron. J.* 71, 333 (1966)] and W. Irvine [*J. Geophys. Res.* 71, 2931 (1966)]. The applicability of these theories is somewhat marginal.
- The exposure age of primary consequence is the cumulative bombardment by meteorites and micrometeorites. The pitting effect of the smaller meteoroids governs roughness in an obvious way, but all bombardment by consolidated rock affects roughness through the deposition of dust particles (with vacuum welding) and larger debris. To the extent that hard radiation may damage crystal structure and, through darkening, may reduce further the significance of higher order scattering of light, the importance of shadowing is enhanced. In both considerations there is a rationale for the Heiligenschein to increase in strength with time.
- For example, if one merely mapped the slope of the relation between brightness increase and phase angle for small phase angles (this was done), the result would show a very strong systematic trend correlated with the variation over the lunar surface of the orientation of the local surface normal with respect to the sunward and earthward average directions. The trend would swamp the variations associated with geologic variety. But it could be removed afterward by d-c plus high-pass spatial filtering of the image.
- The plates used were Eastman Kodak II a-E and 103a-E through a Wratten-4 filter; I took the photographs at the Newtonian focus of the 61-cm reflector of the Northern Arizona University Astrophysical Observatory.
- R. L. Wildey, *Moon* 16, 231 (1977). The method of achieving absolute calibration by normalizing to the total lunar flux is especially important to the need in the present investigation for accurate photometric differences over time.
- The quantity I is also a specific intensity and has the units of heterochromatic power per unit area in a plane perpendicular to the direction of I , per unit solid angle surrounding that direction.
- Power per unit area, appropriately spectrally weighted.
- Normal albedo is the ratio of the observed surface brightness under the condition that $g = i = \epsilon = 0$ to the surface brightness of an ideal surface (Lambertian) which absorbs no energy and presents a directionally invariant specific intensity.
- The angle of incidence is the angle between the

local surface normal and the sunward direction. I have assumed the equivalence of the surface normal and the local vertical.

- The angle of emergence is the angle between the surface normal and the direction to the observer [see also (1)].
- This function is derived from Apollo Heiligenschein photometry as a nominal photometric function for use near zero phase angle only, in which the dependence on i and ϵ has been neglected. It has been published in tabular form by R. Wildey [*Observatory* 96, 235 (1976)]. It varies from a value of 1 at $g = 0^\circ$ to 0.83 at $g = 4^\circ$.
- The ten coefficients, a_n , were determined by the method of least squares in which the set of reduced observations consisting of I for a given selenographic coordinate was used to form the set of all possible ratios of observed I for that coordinate. In this way the quantity ρ disappears when Eqs. 1 and 2 are used to represent the new observational set. The two sets of all such observations on (i) the bright-limb side of the center-of-face and (ii) the terminator side were then formed to provide two separate regions of function definition, within which separate sets of coefficients a_n , obtained from two separate least-square fits, were found. The quantity C was set equal to unity throughout the entire procedure.
- The quantity C was determined by a separate least-square calculation for each selenographic coordinate corresponding to a pixel of the final digital output map. With the a_n already determined, Eqs. 1 and 2 were used directly with the 25 observed values of I to determine ρ and C for each selenographic coordinate.
- In stating that ρ and C are the only terms that are selenographically variable, I exclude, of course, the selenographically correlated variations in g , i , and ϵ that are due to changes in illumination; these variations are fully determined and are not of geologic origin.
- Nevertheless, the form of Eqs. 1 and 2 was not chosen arbitrarily. I originally expected that little, if any, dependence of Φ on i and ϵ would have to be considered, but, when $\Phi = \Phi_0$ was tried, the results were unsatisfactory. It was already known that $\partial\Phi/\partial i$ and $\partial\Phi/\partial\epsilon$ were negligible near $g = 0$, although $\partial\Phi/\partial g$ is about 0.03 to 0.06 per degree. This follows from the fact that the observed Heiligenschein spot retains circular symmetry as it approaches the lunar horizon in Apollo orbital photography [see also (18)]. The determination of C involves such small

brightness differences that $\partial^2\Phi/\partial i\partial g$ and $\partial^2\Phi/\partial\epsilon\partial g$ are nonnegligible. Even these terms had been found small under conditions away from low sun angle and low observing angle [R. Wildey, *NASA Spec. Publ.* 315 (1973)]. The functional form chosen lends itself readily to these properties of the derivatives. It also retains the definitional property whereby $\Phi = 1$ for $g = i = \epsilon = 0$. The reduction to a dependence on $(\cos \epsilon / \cos i)$ is equivalent to a dependence on the single angle called luminance longitude, in keeping with the long-known lunar behavior over the general range of lighting and viewing parameters [see M. Minnaert, in *Planets and Satellites*, G. Kuiper and B. Middlehurst, Eds. (Univ. of Chicago Press, Chicago, 1961), p. 221]. Unfortunately, I found no simple way of achieving these properties while guaranteeing obedience to the reciprocity principle. That was left to its inherent expression in the data and the numerics of a best fit. (The reciprocity principle, which deals with covariance under the interchange of observer and illuminator, is a corollary of the second law of thermodynamics and is discussed by Minnaert.)

- A different effect is the systematic increase in the contrast in C , exemplified by western Oceanus Procellarum as one nears the limb, which was observationally biased in favor of being the bright limb. The result combines with residual shading variations to give the image an appearance of being "lit from the west." I tentatively interpret this to mean that the intrinsic differences in Heiligenschein between different types of terrain genuinely maximizes for low sun and lower observer. This would imply that the Apollo-based observation of the retention of circular symmetry by the Heiligenschein spot on approaching the lunar horizon cannot be generalized with completely adequate precision.
- See Hapke in (3). The present observations support Hapke's prediction of sunward limb-brightening, which earlier observers have not detected.
- Without considerable mobility with regard to the observatory at which the data is gathered, such uniformity for observations extending to small phase angle cannot be achieved except over long periods of time.
- I thank Dr. H. Kieffer, whose very helpful criticism resulted in the complete rewriting of this report. This research was supported by NASA contract W13,130.

12 September 1977; revised 13 January 1978

Oxygen Isotope Composition of Subglacially Precipitated Calcite: Possible Paleoclimatic Implications

Abstract. *Isotopic analyses of subglacially precipitated calcite from near a modern temperate glacier show that the $\delta^{18}\text{O}$ ($= {}^{18}\text{O}/{}^{16}\text{O}$ relative to standard mean ocean water) of the calcite records the $\delta^{18}\text{O}$ of the ice from that glacier. It may therefore be possible to determine the $\delta^{18}\text{O}$ of Pleistocene ice sheets on the basis of isotopic analyses of calcite formed under that ancient ice. This, in turn, would allow estimation of the $\delta^{18}\text{O}$ of Pleistocene oceans and correction of the paleotemperature scale based on foraminiferal oxygen isotopic analyses.*

Thin calcite-rich coatings are widespread on calcareous bedrock exposed by actively retreating temperate glaciers (1). They have been reported near modern glaciers in central Norway (2), the Alps (2, 3), the Rocky Mountains (4, 5), and the Himalayas (5), as well as on bedrock formerly glaciated by the Pleistocene Fennoscandian ice sheet (6). These deposits form by precipitation of CaCO_3 from subglacial waters as a direct consequence of the glacier sliding process (5).

We suggest here that the oxygen isotope composition of calcite that formed under a glacier records the oxygen iso-

tope composition of the ice from that glacier and is relatively independent of the calcite composition of the bedrock. Analyses of calcite precipitated under Pleistocene ice sheets may therefore lead to an estimate of the oxygen isotope composition of the ice sheet. Such an achievement would be of special interest because it could greatly improve the interpretation of apparent foraminiferal paleotemperatures by allowing estimation of the $\delta^{18}\text{O}$ of Pleistocene oceans.

Temperate glaciers slide over their irregular beds by the combined actions of plastic deformation and of pressure melting and refreezing. In the latter process,

which largely controls the chemical regime of subglacial waters (5), ice melts along the up-glacier side of bed obstacles; the resulting water flows through a thin subglacial film to zones of reduced pressure, generally along lee surfaces, where it refreezes (7, 8). The latent heat released by the freezing is conducted through bedrock and ice toward zones of enhanced pressure to provide heat for melting ice. Subglacial waters contain solutes originally present in the basal ice and also solutes derived from the bedrock. As this water refreezes, solutes tend to be systematically rejected into the liquid phase by the growing ice, in much the same way as has been observed in freezing experiments with aqueous solutions of various compositions (5, 9). The solute rejection that is characteristic of freezing, and hence must occur in the sliding process, is therefore responsible for the enrichment and eventual precipitation of solutes in the lee of obstacles overridden by sliding temperate glaciers.

Scattered coatings of subglacial calcite occur in front of retreating temperate glaciers in Glacier National Park, Montana; many of the glaciers lie upon Precambrian carbonate rocks of the Belt series (10). One of the best exposures of subglacial calcites is in the northeast-facing cirque partially occupied by Blackfoot Glacier. This glacier is about 2 km wide and 1.5 km from the upper reaches along the 2900-m-high Continental Divide to the terminus, which was at about 2100 m as of August 1976.

The Helena dolomite and the lower part of the Missoula group (10) are well exposed in the walls and floor of the valley and dip northeastward from 10° to 20°. Examination with a petrographic microscope and a scanning electron microscope shows that the bedrock is predominantly calcite with varying amounts of quartz and minor dolomite, muscovite, and epidote, and that precipitates are almost entirely calcite with minor amounts of detrital quartz. Dolomite is uncommon in the samples of subglacial calcite examined.

In the vicinity of the glacier, the cirque floor is nearly devoid of plant life; owing to the harsh environment and the recency of glacial retreat, even grasses and mosses occur only sporadically in protected areas at the base of low, steep cliffs. Therefore, there is little likelihood of much organically derived CO₂ being incorporated into the meltwater until one is well below the terminus of the glacier.

A meltwater sample taken from a small stream emerging from under the

Table 1. Values of $\delta^{13}\text{C}_{\text{PDB}}$ and $\delta^{18}\text{O}_{\text{SMOW}}$ for bedrock and subglacial calcite and $\delta\text{D}_{\text{SMOW}}$ and $\delta^{18}\text{O}_{\text{SMOW}}$ for ice and meltwater from Blackfoot Glacier (12).

Field number	$\delta^{13}\text{C}_{\text{PDB}}$	$\delta^{18}\text{O}_{\text{SMOW}}$	$\delta\text{D}_{\text{SMOW}}$
<i>Bedrock</i>			
C3	-0.1	+22.4	
D3	+1.6	+20.4	
A2	+1.2	+18.9	
<i>Precipitate</i>			
C3	+0.8	+15.2	
C3	+0.7	+15.9	
A2	-0.1	+15.9	
A5	+1.2	+17.6	
B3	-0.1	+14.9	
B3	-0.2	+14.5	
C4	+0.2	+15.2	
D3	+1.2	+16.7	
<i>Glacier ice</i>			
		-14.8	-113.8
<i>Glacier meltwater</i>			
		-14.6	-113.3

snout of the glacier had the following composition (in milligrams per liter): Ca, 2.9; Mg, 0.3; HCO₃, 10; SO₄, 1.0; SiO₂, 1.1; Fe, 0.02; Na, K, Sr, and Cl, not detected. The field-measured pH was 7.66 ± 0.05. Numerical calculations to test for thermodynamic equilibrium (11) showed that the meltwater was significantly undersaturated with respect to calcite, aragonite, dolomite, and gypsum. However, as explained below, the bulk glacial meltwater is not the same as the solution from which the subglacial calcite is precipitated; the concentration of the solution on the lee side of bedrock obstacles is likely to be 50 to 100 times greater than water derived by melting glacier ice (5).

The stable carbon and oxygen isotope compositions of bedrock and subglacial calcite precipitates from the Blackfoot Glacier area are given in Table 1. The samples analyzed were chosen in a random manner from a large selection of collected samples. The bedrock calcite samples shown in Table 1 have $\delta^{13}\text{C}$ and $\delta^{18}\text{O}$ values (12) typical of Proterozoic carbonate rocks (13). The $\delta^{13}\text{C}$ values of the subglacial calcite precipitates are close to those of the bedrock calcite, but the $\delta^{18}\text{O}$ values of the two types of material are very different, the precipitates being, on the average, about 5 per mil lighter. Some interesting observations can be made from these data. First, the difference in $\delta^{18}\text{O}$ composition confirms that the subglacial calcites are not simply ground-up bedrock calcite (that is, a detrital paste of some sort) but rather that they must have gone through a solution phase. Second, the $\delta^{18}\text{O}$ differences be-

tween bedrock and precipitate imply reequilibration of the oxygen isotopes in the carbonate ligand with another oxygen-bearing reservoir having an isotopic composition not in equilibrium with that of the bedrock calcite. Third, the similarity of $\delta^{13}\text{C}$ values between the two types of material implies that little, if any, organic carbon was involved. The data do not, however, preclude the involvement of atmospheric CO₂.

The $\delta^{18}\text{O}$ of subglacial calcites should clearly reflect the $\delta^{18}\text{O}$ of lee-side water because they form by slow precipitation and hence in isotopic equilibrium with this water. Precipitation of CaCO₃ is accompanied by a preferential incorporation of ¹⁸O in the calcite that corresponds to a fractionation factor of 1.0347 for calcite and water at 0°C (14). Using this factor and the average $\delta^{18}\text{O}$ of +15.7 ± 1.0 per mil for the subglacial calcite (Table 1), we obtain a $\delta^{18}\text{O}$ for lee-side waters of -18.4 ± 1.0 per mil (14).

The isotopic composition of lee-side waters is directly related to that of glacier ice, but the exact relationship, which could significantly affect the $\delta^{18}\text{O}$ deduced for glacier ice by as much as 3 per mil, depends on the nature of the water flow in the subglacial film. Two end-member models of subglacial water flow appear plausible, depending on how most of the water, derived by melting throughout the glacier, flows to the glacier margin. If this bulk meltwater is largely channeled through englacial and subglacial tunnels, much as envisaged by Shreve (15) and Nye (16), the subglacial film would be essentially decoupled from the channelized flow and would accommodate only local down- and up-glacier water flow associated with regelation sliding. We refer to this type of flow (Fig. 1) as local water flow because there is no net down-glacier transfer of water. On the other hand, if most of the meltwater derived throughout the glacier moves and exits through the subglacial film, as favored by Weertman (7), a through flow would exist in the film.

In the through-flow model, we believe that only a small portion of the water that flows through the film would freeze. Because of this and the limited isotopic fractionation characteristic of the freezing process of water (17), the $\delta^{18}\text{O}$ of lee-side water would be practically unaffected by freezing and hence would tend to be identical to that of stoss-side water, which would in turn be identical to the $\delta^{18}\text{O}$ of the glacier ice (18). Using this through-flow model, we estimate that Blackfoot Glacier ice as well as both bulk meltwater and the subglacial film water should generally have a $\delta^{18}\text{O}$ of

-18.4 ± 1.0 per mil and the thin basal layer of regelation ice, which forms by freezing of subglacial film waters, would have a $\delta^{18}\text{O}$ of -15.4 ± 1.0 per mil.

In the local-flow model (that pictured in Fig. 1 for bedslip over a sinusoidal bed), all the water that enters lee areas would freeze there. The selective incorporation of $\delta^{18}\text{O}$ in the growing ice would, therefore, cause the lee-side water in the film to become isotopically lighter. When the $\delta^{18}\text{O}$ of this water becomes lighter by 3 per mil (17, 18) than that of regelation ice, further ^{18}O depletion in the water would cease because the influx of ^{18}O through the flow of water from neighboring stoss surfaces would equal the outflux of ^{18}O through the growth of regelation ice. In this steady-state situation, ice with a $\delta^{18}\text{O}$ of -15.4 ± 1.0 per mil (17) would be in equilibrium with lee-side waters from which calcite formed with the measured range of $\delta^{18}\text{O}$. Because there is negligible net water transfer along the subglacial film for the local-flow model, regelation ice and "normal" glacier ice from the Blackfoot Glacier should have the same $\delta^{18}\text{O}$ of -15.4 ± 1.0 per mil.

Partly because of the complicated water flow associated with glacier sliding over nonsinusoidal beds (19), the actual water flow is likely in general to have characteristics of both through- and local-flow models. We expected, therefore, that on the basis of the average $\delta^{18}\text{O}$ of subglacial calcites from the Blackfoot Glacier area, the $\delta^{18}\text{O}$ of ice from the glacier would range between -15.4 ± 1.0 per mil (local flow) and -18.4 ± 1.0 per mil (through flow). A sample of ice collected near the base of Blackfoot Glacier had a $\delta^{18}\text{O}$ of -14.8 per mil, and a sample of water from one of the meltwater streams emerging from the glacier terminus had a $\delta^{18}\text{O}$ of -14.6 per mil. These two values (Table 1), thought to be suitably representative of the $\delta^{18}\text{O}$ of ice from the lower part of Blackfoot Glacier (20), are in good accord with the value of -15.4 ± 1.0 per mil that we deduced, using the local-flow model to characterize water transport in the subglacial film. These data, therefore, support Shreve's (15) and Nye's (16) concept of glacial hydrology, particularly the notion that the principal function of the film is to accommodate the local flow of water associated with glacier sliding.

We have collected and analyzed several samples of subglacial calcites from the Swiss Alps and the Italian Dolomites. The $\delta^{18}\text{O}$ of the ice from the corresponding glaciers, which we deduced from the calcite $\delta^{18}\text{O}$, are in good agreement with the $\delta^{18}\text{O}$ expected for local precipitation,

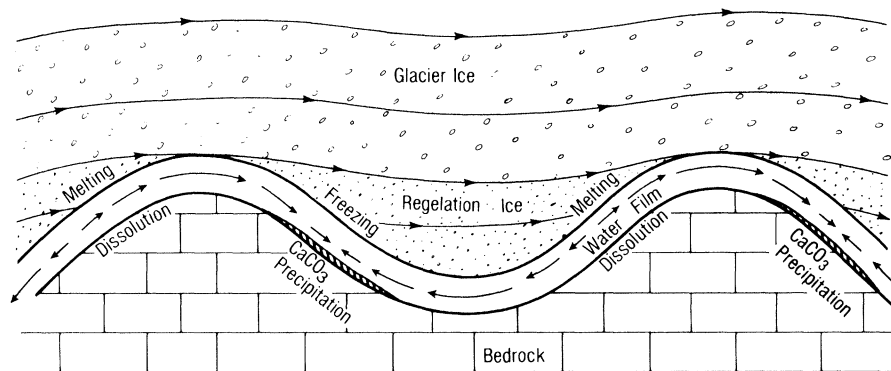


Fig. 1. Schematic diagram of the path lines for temperate ice (ice at the melting point) sliding from left to right over a sinusoidal bed whose wavelength is on the order of several centimeters. Most of the sliding past such small bed undulations takes place by pressure melting and refreezing and the rest by plastic deformation. Water produced by melting in high-pressure areas flows along a thin subglacial film to adjacent zones of lower pressure where it refreezes to form regelation ice. During the freezing process, CaCO_3 and other solutes present in the water are selectively rejected by the growing ice, thereby increasing the solute concentration at the lee of bed obstacles. The solute concentration eventually exceeds the saturation value, and CaCO_3 precipitates subglacially. In this simple situation, water flows up- and down-glacier at varying rates (as indicated by the directions and lengths of arrows) along the subglacial film whose thickness in the figure is greatly exaggerated; in reality, it is probably on the order of micrometers.

as determined from global oxygen isotopic maps (21). Although it will be necessary to sample and analyze ice from several of these European glaciers to confirm this preliminary agreement, it appears that subglacial calcites can indeed effectively record the isotopic composition of the ice from the glacier under which they formed. It also appears that the isotopic composition of subglacial calcites is of special interest to glaciologists because it may yield new insight into the nature of water flow in the subglacial film.

Magaritz (22) studied the isotopic composition of secondary calcites from Mount Hermon, Israel, and from the Austrian Alps. Although the samples he collected in the Alps appear similar to the subglacial calcites we studied, it is difficult to interpret the differences and similarities between his and our isotopic analyses because of major differences in the isotopic composition of the precipitation at his and our study areas.

Our concept is that subglacial calcites precipitate in isotopic equilibrium with the overlying ice and therefore reflect the $\delta^{18}\text{O}$ composition of that ice. We are collecting and analyzing ice, meltwater, calcite bedrock, and precipitates from other temperate glacier areas in Canada and Europe to substantiate our conclusion. We are also searching for locations where subglacial calcite precipitates that formed beneath the continental Pleistocene ice sheets have been preserved. Some of the European localities (2, 3, 6, 23) show promise.

On the basis of the $\delta^{18}\text{O}$ values of planktonic foraminifera from deep-sea

cores, Emiliani (24) has constructed a paleotemperature curve for Atlantic equatorial surface waters that is widely used in paleoclimate modeling. Dansgaard and Tauber (21) have pointed out that as much as 70 percent of Emiliani's "temperature" curve may in fact be caused by an isotopic shift of the oceans. In other words, instead of equatorial surface waters being cooler by 7°C during glacial maxima, they may have been cooler by only 2°C than today. The problem is to determine what the $\delta^{18}\text{O}$ content of the ice sheets really was and thus correct the $\delta^{18}\text{O}$ foraminiferal paleotemperature scale.

BRUCE B. HANSHAW

*U.S. Geological Survey,
National Center, Mail Stop 431,
Reston, Virginia 22092*

BERNARD HALLET

*Department of Geology,
Stanford University,
Stanford, California 94305*

References and Notes

1. Temperate glaciers are those that are at their melting point throughout, except for a surface layer that freezes during the winter.
2. L. Samuelsson, *Geol. Foeren. Stockholm Foerh.* **85**, 414 (1964).
3. V. F. Bauer, *Z. Gletscherkd. Glazialgeol.* **4** (No. 3), 215 (1961).
4. D. C. Ford, P. G. Fuller, J. J. Drake, *Nature (London)* **226**, 441 (1970).
5. B. Hallet, *Geol. Soc. Am. Bull.* **87**, 1003 (1976). The solution used in these experiments contained CaCO_3 . Hallet found subglacial calcites in the Himalayas, but these have not yet been described in the literature.
6. L. E. Kers, *Geol. Foeren. Stockholm Foerh.* **86**, 282 (1964); T. Bjaerke and H. Dypvik, *J. Sediment. Petrol.* **47**, 1321 (1977).
7. J. Weertman, *J. Glaciol.* **3**, 33 (1957).
8. W. B. Kamb, *Rev. Geophys. Space Phys.* **8**, 673 (1970).
9. J. P. Terwilliger and S. F. Dizio, *Chem. Eng. Sci.* **25**, 1331 (1970); G. Kvajic and V. Brajovic, *J. Cryst. Growth* **11**, 73 (1971); R. G. Seiden-

- sticker, *J. Chem. Phys.* **56**, 2853 (1972). The solutions used in the above experiments contained, respectively, NaCl, KOH, and HCl.
- C. P. Ross, *U.S. Geol. Surv. Prof. Pap.* **296** (1959).
 - L. N. Plummer, B. F. Jones, A. H. Truesdell, *U.S. Geol. Surv. Water Res. Invest.* **76-13** (1976). This paper presents a computer program for calculating chemical equilibrium between solutes in natural water and rock-forming minerals.
 - The δ values are defined as

$$\delta = \left(\frac{R_{\text{sample}}}{R_{\text{standard}}} - 1 \right) \times 1000$$

- where for $\delta^{13}\text{C}$, $R = {}^{13}\text{C}/{}^{12}\text{C}$; for $\delta^{18}\text{O}$, $R = {}^{18}\text{O}/{}^{16}\text{O}$; and for δD , $R = \text{D}/\text{H}$. The standard for carbon isotopes is Pee Dee belemnite (PDB); the standard for oxygen and hydrogen isotopes is standard mean ocean water (SMOW).
- J. Veizer and J. Hoefs, *Geochim. Cosmochim. Acta* **40**, 1387 (1976).
 - R. N. Clayton, B. F. Jones, R. A. Berner, *ibid.* **32**, 415 (1968). Our value for the isotopic composition of lee-side water is calculated from the relationship

$$\frac{({}^{18}\text{O}/{}^{16}\text{O})_{\text{calcite}}}{({}^{18}\text{O}/{}^{16}\text{O})_{\text{water}}} = 1.0347 = \frac{1 + \frac{15.7}{1000}}{1 + \frac{x}{1000}}$$

- where x is the $\delta^{18}\text{O}$ of lee-side water.
- R. L. Shreve, *J. Glaciol.* **11**, 205 (1972).
 - J. F. Nye, paper presented at the Union Géodésique et Géophysique Internationale-Association Internationale d'Hydrologie Scientifique-Commission de Neiges et Glaces Symposium on the Hydrology of Glaciers, Cambridge, England, 7-13 September 1969; *J. Glaciol.* **17**, 181 (1976).
 - We use the ice-water fractionation factor deter-

mined by O'Neil to be 1.003 for ${}^{18}\text{O}/{}^{16}\text{O}$ [J. R. O'Neil, *J. Phys. Chem.* **72**, 3683 (1968)].

$$\frac{({}^{18}\text{O}/{}^{16}\text{O})_{\text{calcite}}}{({}^{18}\text{O}/{}^{16}\text{O})_{\text{ice}}} = \frac{1.0347}{1.003} = 1.0316$$

- Here we assume negligible oxygen isotope fractionation upon melting; we intend to check this experimentally.
- J. F. Nye, in *Physics and Chemistry of Ice*, E. Whalley, S. J. Jones, L. W. Gold, Eds. (Royal Society of Canada, Ottawa, 1973), pp. 387-394.
- We plan more systematic and comprehensive sampling of the ice to document possible spatial variations in the isotopic composition of Black-foot Glacier ice. Spatial variations in $\delta^{18}\text{O}$ of several per mil have been reported for Saskatchewan Glacier ice by S. Epstein and R. P. Sharp [*J. Geol.* **67**, 88 (1959)].
- W. Dansgaard and H. Tauber, *Science* **166**, 499 (1969).
- M. Magaritz, *Earth Planet. Sci. Lett.* **17**, 385 (1973).
- Y. A. Lavrushin and N. V. Rengarten, *Litol. Polezn. Iskop.* **6**, 21 (1974).
- C. Emiliani, *J. Geol.* **63**, 538 (1955); *Science* **154**, 851 (1966); S. Gartner and C. Emiliani, *Am. Assoc. Petrol. Geol. Bull.* **60**, 1562 (1976).
- We thank T. Coplen, W. Dansgaard, D. Ford, I. Kaplan, K. Krauskopf, M. Meier, J. Nye, R. Shreve, T. Wigley, and I. Winograd for stimulating discussions and manuscript criticism. We also thank R. Goldthwait for locating Pleistocene-age subglacial precipitate areas for us in Ohio. We especially thank J. Woodward and T. Coplen for the stable isotope analyses. We are grateful for the help of R. Frauson of the U.S. National Park Service in gaining access to the study areas. Part of this report was presented at the Second International Symposium on Water-Rock Interaction, Strasbourg, France, 17-25 August 1977.

7 October 1977; revised 1 February 1978

Excitation-Contraction Coupling in Skeletal Muscle: Blockade by High Extracellular Concentrations of Calcium Buffers

Abstract. *High concentrations (80 to 90 millimolar) of the calcium buffers EGTA and citrate (less than 10^{-7} molar free calcium ion) reversibly block excitation-contraction coupling in intact frog skeletal muscle fibers, but do not block caffeine-induced contractures. Solutions containing the same free calcium concentration but lower concentrations of calcium buffer (1 millimolar) do not block excitation-contraction coupling. These results suggest that excitation-contraction coupling requires the presence of calcium in a "protected" extracellular compartment, probably the transverse tubular network, and that calcium is actively transported into this compartment from the muscle cell cytoplasm.*

There has been considerable debate over whether extracellular calcium is essential for excitation-contraction coupling in skeletal muscle. The following proposed mechanism for excitation-contraction coupling (1, 2) assigns a central role to extracellular calcium: the muscle action potential depolarizes the transverse tubules, increasing their calcium permeability, and the resultant flux of calcium from the transverse tubular lumen into the myofilament space either directly or indirectly induces release of calcium stored in the terminal cisternae of the sarcoplasmic reticulum. This hypothesis fell into disfavor with the demonstration that excitation-contraction coupling persists in solutions containing no added calcium plus 1 mM of the calcium buffer, ethylene glycol bis(β -aminoethyl ether)-*N,N,N',N'*-tetraacetic

acid (EGTA) (free $[\text{Ca}^{2+}] < 10^{-8}\text{M}$) [see (3)].

However, we suggest that 1 mM EGTA does not remove all free calcium from the transverse tubular system, since diffusion within this narrow convoluted system is almost certainly restricted (4) and since transverse tubular membranes may actively transport calcium (5). We demonstrate here that higher bath concentrations (80 to 90 mM) of the calcium buffers EGTA and citrate (free $[\text{Ca}^{2+}] < 10^{-7}\text{M}$) do reversibly block excitation-contraction coupling in frog skeletal muscle. These results strongly suggest that excitation-contraction coupling requires the presence of Ca^{2+} in some "protected" extracellular compartment, and are compatible with the hypothesis that calcium release from the sarcoplasmic reticulum is normally dependent on

calcium influx across transverse tubular membranes.

Single muscle fibers were dissected from the cutaneous pectoris muscle of small grass frogs (*Rana pipiens*). An isolated muscle fiber was impaled with two micropipettes filled with 0.2M K_2SO_4 ; one pipette injected current, the other recorded transmembrane potential. Action potentials were evoked by applying pulses of depolarizing current. In solutions where the resting membrane potential was depolarized, the depolarizing current pulses were superimposed on a steady hyperpolarizing current. Contractions of the impaled muscle fiber were monitored visually (at 600 \times), and were also apparent as movement artifacts in the voltage record. The normal Ringer solution contained 120 mM NaCl, 2.5 mM KCl, and 1.8 mM CaCl_2 . In modifications of this Ringer solution all or part of the calcium was omitted and sodium EGTA, sodium citrate, Na_2SO_4 , tetramethylammonium chloride, or sucrose was isotonicly substituted for all or part of the NaCl. All solutions were adjusted to pH 7.2 to 7.3, using PIPES (1.4-piperazinediethanesulfonic acid) or citrate as an H^+ buffer and phenol red (5 mg/liter) as a pH indicator. Most solutions contained 2.5 mM K^+ and 0.5 g of glucose per liter. Experiments were performed at 15° to 20°C.

In agreement with earlier studies (3), we found that Ringer solutions containing 1 mM EGTA and no added calcium (free $[\text{Ca}^{2+}] < 10^{-8}\text{M}$) did not block excitation-contraction coupling in isolated muscle fibers. Contractions continued for as long as action potentials could be evoked, usually 20 to 30 minutes. However, when the concentration of EGTA was increased to 85 mM (an isotonic solution of sodium EGTA), or when the solution contained isotonic sodium citrate (82 to 90 mM), action potentials evoked by applied current were no longer followed by contractions. The solutions with high concentrations of buffer and low $[\text{Ca}^{2+}]$ depolarized the muscle fibers, and it was usually necessary to hyperpolarize the fibers before action potentials could be evoked. Figure 1 shows a muscle action potential recorded in 82 mM citrate; the action potential has a nearly normal amplitude (80 mV), but it evoked no visible contraction, and no mechanical artifact was evident in the voltage trace. Similar results were obtained in single fiber preparations from more than ten different muscles bathed in isotonic sodium citrate (6). The high [buffer]-low $[\text{Ca}^{2+}]$ solutions reduced the apparent input resistance of the muscle fibers (7), and solutions containing less